

25<sup>th</sup> ABCM International Congress of Mechanical Engineering  
October 20-25, 2019, Uberlândia, MG, Brazil

**COB-2019-0673**

## **TURBOCHARGER TURBINE DIFFUSER WALL SHAPE OPTIMISATION**

**José Arthur Gonçalves da Silva Teixeira**<sup>1,2</sup>

**Bryan Castro Caetano**<sup>1,2</sup>

**Matheus Ungaretti Borges**<sup>1</sup>

**Jose Guilherme Coelho Baêta**<sup>1,2</sup>

**Ricardo Poley Martins Ferreira**<sup>1</sup>

<sup>1</sup>Programa de Pós-Graduação em Engenharia Mecânica, Universidade Federal de Minas Gerais, Brazil

<sup>2</sup> Centro de Tecnologia da Mobilidade, Universidade Federal de Minas Gerais, Brazil

jose.arthur.gst@gmail.com

bcastrocaetano@gmail.com

matheusungaretti@gmail.com

baeta@demec.ufmg.br

poley@demec.ufmg.br

**Abstract.** Supercharging has been increasingly more employed as an approach to improve the powertrain energy efficiency. The turbocharger stands out as a well-established technology which recovers waste energy from exhaust gases to increase the engine intake pressure and mass flow rate. Therefore, the reduction of the pressure downstream the rotor can be a valid way to improve turbocharger performance, since it entails in a larger pressure drop across the turbine. Diffusers are devices that can be used to further reduce the rotor outlet pressure. Diffuser wall parametrisation can be achieved by using polynomial functions with enforced analytically derived constraints of monotonicity. The present study aimed to maximise the static pressure recovery of a polynomial parametrised radial turbine diffuser of an automotive turbocharger. A series of CFD analyses were carried out in order to obtain the pressure recovery coefficient of a conical and a set of parametrised diffusers. An optimal parametrised diffuser was determined using a genetic algorithm and sequential quadratic programming hybrid optimisation algorithm by maximising the pressure recovery coefficient. Finally, the flow lines and the pressure distribution of the conical and the optimal diffuser were described.

**Keywords:** Turbocharger, Diffuser, CFD, Genetic Algorithm, Sequential Quadratic Programming

### **1. INTRODUCTION**

Currently, the recurrent energy crises and the alarmingly crescent environmental pollution became a concern of all spheres of society. More than one third of the total energy consumption in industrialised countries is due to transportation. Thus, vehicles became rather important study object for energy consumption and emissions reduction (Fu *et al.*, 2014). Nowadays, the focus of engine research is mainly on two fronts: the development and employment of alternative fuels and the improvement of energy harnessing and recovery (Fu *et al.*, 2013).

In this scenario, turbocharging became a technology of great importance in the automotive industry. Already established in compression ignition engines, this equipment has a crescent growing in spark ignited engines in recent decades. Hence, that growth became the fuel for the development of many improvements in technology (Galindo *et al.*, 2013). The turbocharger consists of a compressor driven by a radial turbine, where energy is recovered from the exhaust gases, mainly through exhaust pressure drop. Therefore, reducing the pressure downstream the rotor can be a valid way to improve the efficiency of those equipment.

Diffusers are devices that reduce the velocity and increase the static pressure of a fluid passing through it. Thus, for a given exit pressure, a greater pressure recovery implies a lower pressure upstream in the diffuser. Diffuser wall parametrisation can be achieved by using polynomial functions or parametric curves such as B-splines and Bezier curves. Although polynomials are often considered impractical for design optimisation due to a tendency to produce undesirable wiggles, this problem can be mitigated by enforcing analytically derived constraints of monotonicity (Madsen *et al.*, 2000a).

One method to find the optimal solution is the use of optimisation algorithms, such as Genetic Algorithms (GA) and Sequential Quadratic Programming (SQP), to maximise the pressure recovery coefficient. According to Mühlbein *et al.* (1991), the GA are informally described as follows: subgroups of individuals (set of vectors) live on a ladder-like world; new offspring are created by genetic operators within a subpopulation; every  $k$  generations, the best individual of

a subpopulation is sent to its neighbours. The GA begin its search from a randomly generated population that evolve over successive generations, eliminating the need for a user-supplied starting point (Hassan *et al.*, 2005). The phenotype of an individual is given by a real vector  $x$ , and the genotype of an individual is given by the bit representation  $y$  of  $x$  according to the floating-point format (Mühlenbein *et al.*, 1991).

Notwithstanding the capability of find the global optimal region, zero-order algorithms are not as computationally efficient as gradient-based algorithms. The SQP is a popular-general purpose optimisation algorithm that creates an approximate quadratic programming sub-problem that is used to find a search direction. However, SQP algorithm may not converge to a global optimum if started far from the solution (Venter and Vanderplaats, 2009). This method replaces the original problem by a sequence of quadratic programming problems which are exactly solvable, and which approximate the original one (Abdo and Rackwitz, 1991).

Henceforth, the objective of the present study was to maximise static pressure recovery of a polynomial parametrised radial turbine diffuser of an automotive turbocharger. Computational Fluid Dynamics (CFD) simulation was carried out in order to obtain the diffuser pressure recovery coefficient of a conical and a set of parametrised diffusers. An optimal parametrised diffuser was determined using a hybrid optimisation algorithm, consisted of GA and SQP, to maximise the pressure recovery coefficient. Finally, the flow lines and the pressure distribution of the conical and the optimal diffuser were analysed.

## 2. METHODOLOGY

The methodology employed to optimise the diffuser shape is highlighted in the following subsections. Firstly, the wall parametrisation is described presenting the wall shape function and its monotonic constraint. Subsequently, the CFD simulation strategy is depicted disclosing the geometrical and the numerical models and the simulation boundary conditions. Finally, the diffuser wall optimisation approach is defined presenting the optimisation algorithm utilised and the objective function.

### 2.1 Diffuser Parametrisation

A polynomial function was chosen to represent the diffuser contour since it is a simple curve representation. The profile of a polynomial parametrised diffuser is exemplified in Fig. 1. The shape of the diffuser wall is described by a function  $y(x)$ , in which  $y$  denotes the vertical position of wall points, being  $y(0) = 0$  at inlet and  $y(x_f) = y_f$  at outlet.

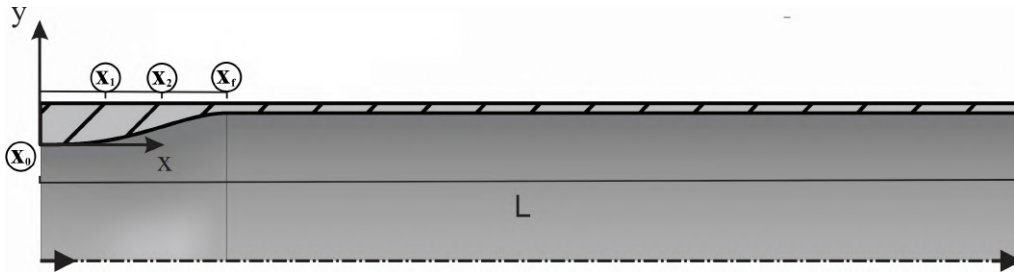


Figure 1: Parametrised diffuser profile.

The independent variable  $x$  is the axial position along the curved wall, being  $0 \leq x \leq x_f$ ,  $x = 0$  at inlet and  $x = x_f$  at outlet of the curved section. The two-design-variable wall contour was defined by a fourth-order polynomial:

$$y(x) = a_4x^4 + a_3x^3 + a_2x^2 + a_1x + a_0 \quad (1)$$

The vertical positions of two control points are the design variables in which the curve must pass through at  $x_1$  and  $x_2$ . Given four points of the curve (inlet, outlet and the two control points  $x_1$  and  $x_2$ ) and the condition of zero slope, i.e.  $dy/dx = 0$ , at the diffuser inlet, the polynomial function reduces to:

$$y(x) = a_4x^4 + a_3x^3 + a_2x^2 \quad (2)$$

Solving Eq. 2 for  $x_1$ ,  $x_2$  and  $x_f$ , the polynomial coefficients are obtained as described in Eq. 3:

$$a_2 = \frac{108y_1 - 27y_2}{4x_f^2} + \frac{y_f}{x_f^2}; \quad a_3 = \frac{-135y_1 + 54y_2}{2x_f^3} - \frac{9y_f}{2x_f^3}; \quad a_4 = \frac{162y_1 - 81y_2}{4x_f^4} + \frac{9y_f}{2x_f^4}. \quad (3)$$

Experimental and numerical evidences indicate that maximum pressure recovery in diffusers occurs at the border of appreciable flow separation. Thus, strongly separated flows should be avoided, which makes reasonable to restrict the designs to monotonic wall shapes, as mentioned by Madsen *et al.* (2000a). The monotonicity in the position of control

points yields Eq. 4:

$$0 \leq y_1 \leq y_2 \leq y_f \quad (4)$$

Finally, according to Djebedjian (2004), a wall shape is monotonic when the first-order derivative is greater than zero:

$$\frac{dy}{dx} = x(4a_4x^2 + 3a_3x + 2a_2) > 0 \quad (5)$$

Considering:

$$Z(x) = 4a_4x^2 + 3a_3x + 2a_2 \quad (6)$$

Then:

$$\frac{dy}{dx} = xZ(x) > 0 \quad (7)$$

Since  $x$  is positive throughout the domain, it is enough that the Eq. 6 is greater than 0 for the Eq. 7 be positive. Solving Eq. 6 for  $x_0$  and  $x_f$ :

$$y_2 \leq 4y_1 + \frac{4}{27}y_f \quad (8)$$

$$y_2 \leq y_1 + \frac{13}{27}y_f \quad (9)$$

## 2.2 CFD Simulation

The pressure recovery coefficient of a pool of ten sampling geometries within the monotonicity constraint domain and of a conical diffuser was obtained with aid of the CFD solver ANSYS CFX<sup>®</sup>. This software makes use of an element-based finite volume method in which the geometric domain of the fluid is discretized in a mesh. Then, the conservative form of Navier-Stokes state equations for are solved for every element in the fluid domain. The flow of air across a Biagio turbocharger radial turbine was numerically simulated in steady state, with a frozen rotor at 100 krpm, considering as heat transfer and turbulence models respectively total energy and k- $\epsilon$ . Figure 2 shows the computational domain.

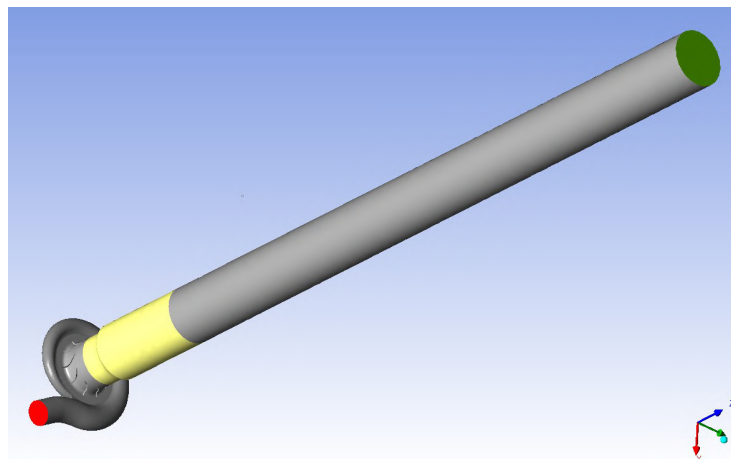


Figure 2: Simulated model.

The volute inlet, i.e. the red surface in the volute region, was considered the domain inlet with the average mass flow and temperature of a 1.4 L petrol engine at 5500 rpm and full load. The rotor outlet was connected to the diffuser domain, i.e. the yellow volume downstream the rotor. The diffuser domain had 100 mm and consisted of the diffuser section, with 20 mm for the conical and 19 mm for the parametrised cases, and a straight section of the terminal diameter of 44.45 mm, this diameter being the same as the exhaust pipe of a given turbocharger application. The diffuser section was connected to a straight pipe of length ten times greater than the rotor exducer diameter. This approach was taken in order to ensure complete flow development at the diffuser. The outlet, i.e. the green surface in the straight section, was considered to be at atmospheric pressure. The configuration of the CFD case is summarised in Tab. 1.

Table 1: CFD case setting.

<b>Simulation models</b>	
Heat Transfer Model	Total Energy
Turbulence Model	k- $\epsilon$
<b>Mesh Elements</b>	
Volute	39091
Rotor	75296
Diffuser	94468
Exhaust Pipe	35918
Total	244773
<b>Convergence Control</b>	
Timescale Control	Auto Timescale
Length Scale Option	Aggressive
Residual Target	$1.0 \times 10^{-5}$ RMS
<b>Boundary Conditions</b>	
Inlet	Mass Flow Rate: 0.07602 kg/s
	Total Temperature: 870 K
Rotor	Rotor Speed: 100000 rpm
	Interfaces: Frozen Rotor and Rotational Periodicity
Outlet	Average Static Pressure: 101.325 kPa

### 2.3 Optimisation Strategy and Objective Function

This study was performed using a hybrid optimisation algorithm, mixing a zero-order and a gradient-based procedure. Firstly, a GA search was performed to approach the global optimal region. Then, SQP was started to faster convergence to the local optimum. The optimisation algorithm was set with the configuration shown in Tab. 2.

Table 2: Optimisation algorithm settings utilised.

<b>GA Configuration</b>	
Elite count	10
Population size	200
Function tolerance	$1 \times 10^{-10}$
Crossover function	Scattered
Fitness Scaling function	Rank Scaling
Mutation function	Gaussian
<b>SQP Configuration</b>	
Optimality tolerance	$1 \times 10^{-100}$
Constraint tolerance	$1 \times 10^{-100}$

The working principle of the diffuser is to obtain a static pressure rise through deceleration of the fluid by enlarging the cross-section area. Depending on the particular diffuser installation, the primary objective can be either to decrease velocity, to increase pressure or to supply a downstream process with a steady uniform flow (Djebedjian, 2004). Being of interest of energy recovery to minimise the rotor exit pressure, the objective of the proposed diffuser was to maximise static pressure rise.

The diffuser performance is characterised by the static pressure recovery. The static pressure recovery coefficient  $C_p$  can be defined as described in Eq. 10:

$$C_p = \frac{\Delta p}{0,5\rho U_{in}^2} \quad (10)$$

in which,  $\Delta p$  is the difference between the static pressures at the diffuser domain outlet and inlet,  $\rho$  is the air average specific mass and  $U$  is the inlet velocity (Madsen *et al.*, 2000a). The  $C_p$  results for the parametrised diffusers were then fitted in function of the diffuser design parameters through a two-variable third-order polynomial:

$$C_{p,est} = c_0 + c_1y_1 + c_2y_2 + c_3y_1^2 + c_4y_2^2 + c_5y_1y_2 + c_6y_1^3 + c_7y_2^3 + c_8y_2y_1^2 + c_9y_1y_2^2 \quad (11)$$

Thus, the objective of the optimisation problem was to maximise the diffuser's pressure recovery,  $C_{p,est}$ , adjusting

the width of two cross-sectional area which are fixed in the diffuser length,  $y_1$  and  $y_2$ . Finally, the diffuser geometry is limited by three functional constraints, described by Eqs. 4, 8 and 9. The optimisation problem is summarised in Tab. 3.

Table 3: Summary of optimisation problem.

<b>Objective function</b>	Eq. 11
<b>Parameters</b>	$y_1$ and $y_2$
<b>Design constraints</b>	Eqs. 4, 8 and 9.

### 3. RESULTS

In order to study the correlation of the recovery pressure with the geometric parameters, ten parametrised samples of 19 mm and a conical diffuser of 20 mm were simulated. Equation 10 was implemented as a custom expression in ANSYS CFD Post-processing<sup>®</sup>. With the simulated results of  $C_p$  for the parametrised diffusers, exhibited in Tab. 4, the coefficients  $c_i$  of the Eq. 11 were obtained, being the resultant coefficients are disposed in Tab. 5. The domain of values of  $y_1$  and  $y_2$  and the resultant  $C_p$  surface are shown in Fig. 3. The feasible diffuser designs are enclosed in the area above Eq. 4, represented as solid line, and under Eqs.8, dashed line, and 9, dash-dot line.

Table 4: Numeric simulation results.

$y_1$	0.0000	0.0000	0.3583	1.6722	3.2250	1.6722	0.3583	0.1792	0.3583	1.6722
$y_2$	0.0000	0.4778	1.9111	3.2250	3.2250	1.6722	0.3583	0.4778	1.1347	2.4486
$C_p$	0.8186	0.8173	0.8054	0.7938	0.7741	0.7945	0.8151	0.8149	0.8139	0.8000

Table 5: Eq. 10 coefficients attained with the simulated parametrised diffusers.

$c_i$	$c_0$	$c_1$	$c_2$	$c_3$	$c_4$	$c_5$	$c_6$	$c_7$	$c_8$	$c_9$
Value	0.8186	0.0058	- 0.0137	0.0293	0.0298	- 0.0653	0.0066	- 0.0150	- 0.0325	0.0423

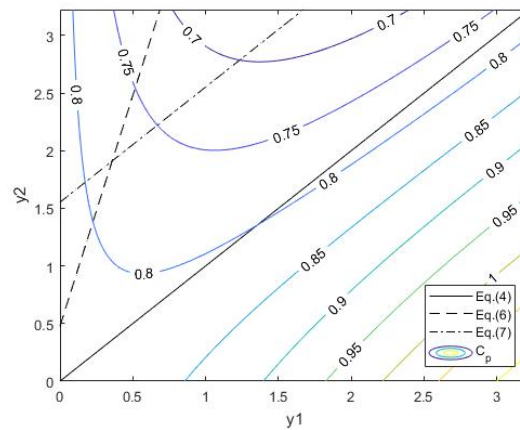


Figure 3: Response surface and design constraints.

The GA optimisation terminated within 100 generations, achieving an average change of fitness value lesser than the defined function tolerance. The SQP optimisation completed with three iterations, with the function being non-decreasing in the feasible directions around the achieved solution. Furthermore, the optimality tolerance was satisfied within the defined value of constraint tolerance. The hybrid optimisation algorithm found an optimum  $C_{p,est}$  of 0.8186 for a 19 mm diffuser of  $y_1 = 0$  and  $y_2 = 0$  versus a  $C_p$  of 0.8131 of the conical diffuser. This small gain is coherent with the findings that the pressure recovery improves marginally for small area ratios (Madsen *et al.*, 2000b). Even so, for an area ratio of 1.17 an improvement of 0.67% was obtained.

The pressure profiles obtained in the numerical simulation are exposed in Fig. 4. In both cases, a low-pressure region is noticed at the first half of the diffuser length. This phenomenon, known as separation bubble, can be attributed to the abrupt end of the turbine rub wall, which leads to a backward facing step with separation and flow recirculation downstream the turbine axle (Volkmer *et al.*, 2012). This region can be attributed to the end of the turbine axle, which

extends for 14.80 mm downstream the rotor on the real turbocharger turbine. Nevertheless, it is notorious that such low-pressure zone is bigger for the conical diffuser than for the parameterised counterpart. In addition, the optimal diffuser shown a tendency to sustain the pressure rise afterwards its region. The conical diffuser, however, exhibited an abrupt pressure rise shortly after its inlet, almost reaching terminal pressure at the diffuser outlet.

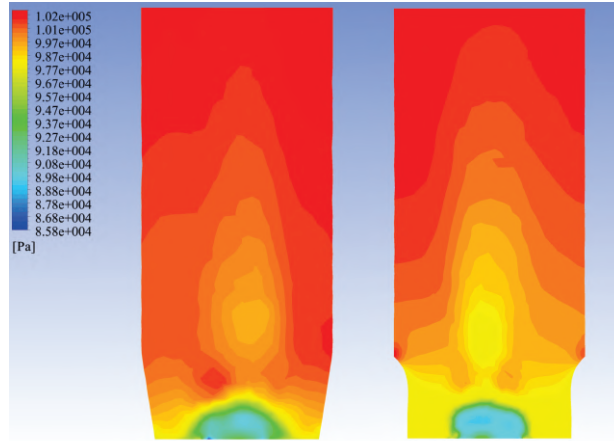


Figure 4: Pressure profile obtained by conical (left) and optimal (right) diffuser.

The pressure rise through the diffuser region of both cases is detailed in Fig. 5. It is noticeable the abrupt pressure rise in the conical diffuser, having high-pressure regions halfway its length. In other hand, the pressure raise came out to be delayed in the optimal diffuser.

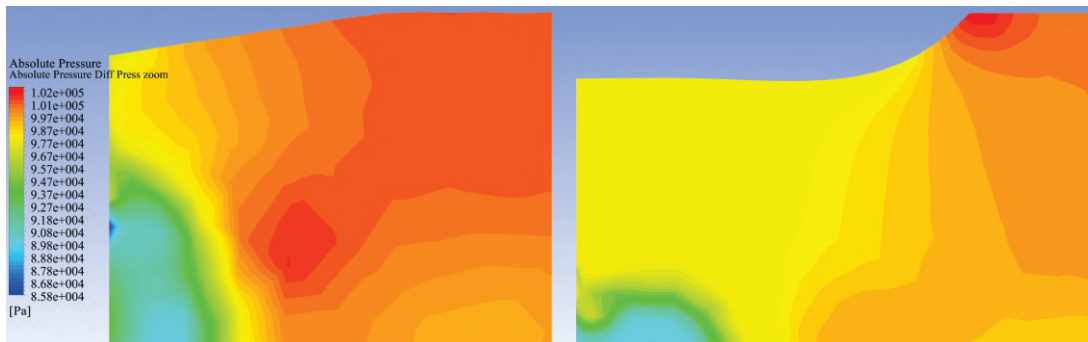


Figure 5: Pressure rise on conical (left) and optimal (right) diffuser.

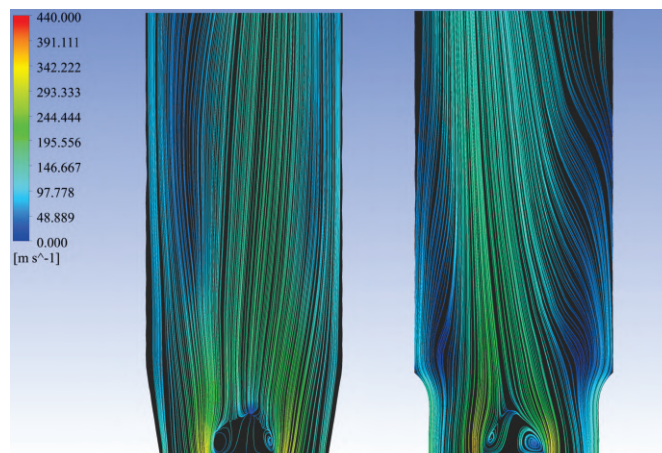


Figure 6: Flow observed on conical (left) and optimal (right) diffuser.

The flow profile obtained in the simulations are exposed Figure 6. In both cases, it is clear the presence of the aforementioned separation bubble in the centre of the diffuser inlet. This phenomenon can lead to a strong hub wake with high losses in the centre of the diffuser. The interaction between the end of the hub and the downstream diffuser can have a significant influence on diffuser flow field and hence on overall gas turbine performance (Volkmer *et al.*, 2012).

Moreover, the separation bubble for the conical diffuser flow turn up rather non-uniform, whereas the bubble shape for the optimal diffuser was akin to a streamlined body. That format indicates that the optimal diffuser better mitigated the efficiency loss of the flow when compared with the conical diffuser.

The flow near the diffuser wall is evidenced in Fig. 7. It is notorious the flow separation from the wall around one fifth of the conical diffuser length, which is an indication of poor performance of an aerodynamic surface. In contrast, the optimal diffuser had not a considerable flow separation the wall in almost all its length. The outward bent shape indicates that the optimisation adjusted the wall slope to delay the flow separation as far as possible, avoiding large losses.

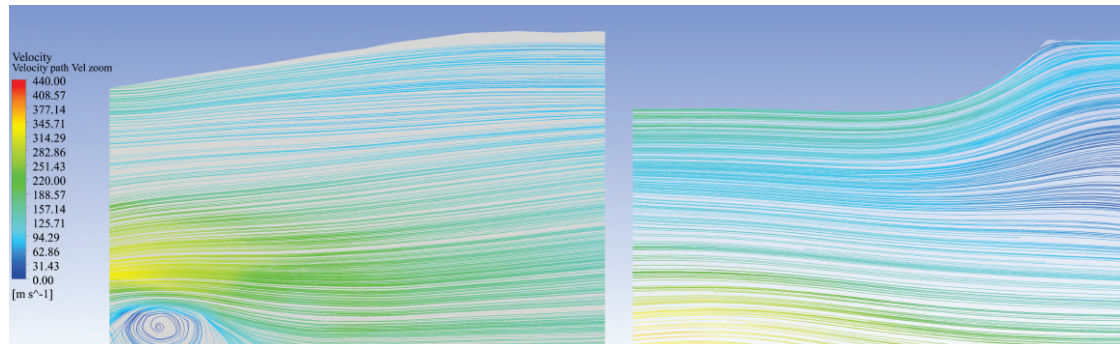


Figure 7: Flow near the wall of conical (left) and optimal (right) diffuser.

#### 4. CONCLUSION

This study used polynomial approximation for wall shape optimisation. The shape of the wall was optimised in order to achieve maximum pressure recovery. The static pressure recovery coefficient  $C_p$  was parametrised for two design variables and fitted with the result of ten random simulated samples within the feasible design domain. In order to achieve a fast convergence to the global optimum, this study deployed a hybrid optimisation algorithm, mixing zero-order and gradient based approaches, namely Genetic Algorithm and Sequential Quadratic Programming.

The mixed optimisation algorithm worked smoothly, finding the optimal geometry within few iterations for the given model. This strategy proved to be successful to neutralise two of the biggest drawbacks of each approach, improving the convergence precision while allowing to start the optimisation without knowing the circa optimum region. Furthermore, the diffuser wall shape parametrisation in function of the width of two length fixed points and monotonic constrained proved to be rather efficient, allowing the convenience and low computational costs. Finally, the diffuser performance was successfully improved by wall contouring.

Although the improvement turned up to be marginal due to small area ratio analysed, one ought to consider that the approach presented in this study can be easily applied for cases with greater area ratios. Also, considering the delay of the pressure rise of the cross-sectional area for the optimal diffuser, further analyses could be carried considering the optimal position lengthwise for the optimal vertical position.

#### 5. ACKNOWLEDGEMENTS

This study was financed in part by the Coordenação de Aperfeiçoamento de Pessoal de Nível Superior - Brazil (CAPES) - Finance Code 001

#### 6. REFERENCES

- Abdo, T. and Rackwitz, R., 1991. "A new beta-point algorithm for large time-invariant and time-variant reliability problems". In *Reliability and Optimization of Structural Systems' 90*, Springer, pp. 1–12.
- Djebedjian, B., 2004. "Two-Dimensional Diffuser Shape Optimization." *Proceedings of IMEC2004, International Mechanical Engineering Conference*, pp. 1–19.
- Fu, J., Liu, J., Xu, Z., Ren, C. and Deng, B., 2013. "A combined thermodynamic cycle based on methanol dissociation foric (internal combustion) engine exhaust heat recovery". *Energy*, Vol. 55, pp. 778 – 786. ISSN 0360-5442. doi: <https://doi.org/10.1016/j.energy.2013.04.026>.
- Fu, J., Tang, Q., Liu, J., Deng, B., Yang, J. and Feng, R., 2014. "A combined air cycle used for ic engine supercharging based on waste heat recovery". *Energy Conversion and Management*, Vol. 87, pp. 86 – 95. ISSN 0196-8904. doi: <https://doi.org/10.1016/j.enconman.2014.06.097>.
- Galindo, J., Fajardo, P., Navarro, R. and García-Cuevas, L., 2013. "Characterization of a radial turbocharger turbine in pulsating flow by means of cfd and its application to engine modeling". *Applied Energy*, Vol. 103, pp. 116 – 127. ISSN 0306-2619. doi: <https://doi.org/10.1016/j.apenergy.2012.09.013>.

- Hassan, R., Cohanin, B., de Weck, O. and Venter, G., 2005. "A Comparison of Particle Swarm Optimization and the Genetic Algorithm". *46th AIAA/ASME/ASCE/AHS/ASC Structures, Structural Dynamics and Materials Conference*. ISSN 2005-1897. doi:10.2514/6.2005-1897.
- Madsen, J.I., Shyy, W. and Haftka, R.T., 2000a. "Response Surface Techniques for Diffuser Shape Optimization". *AIAA Journal*, Vol. 38, No. 9, pp. 1512–1518. ISSN 0001-1452. doi:10.2514/2.1160.
- Madsen, J.I., Olhoff, N. and Condra, T.J., 2000b. "Optimization of straight, two-dimensional diffusers by wall contouring and guide vane insertion". *Proceedings of the 3rd World Congress of Structural and Multidisciplinary Optimization, Wcsmo-3, May 17-21, 1999, State University of New York at Buffalo, Buffalo, New York*.
- Mühlenbein, H., Schomisch, M. and Born, J., 1991. "The parallel genetic algorithm as function optimizer". *Parallel Computing*, Vol. 17, No. 6-7, pp. 619–632. ISSN 01678191. doi:10.1016/S0167-8191(05)80052-3.
- Venter, G. and Vanderplaats, G.N., 2009. "Using a Filter-Based SQP Algorithm in a Parallel Environment". *50th AIAA/ASME/ASCE/AHS/ASC structures, Structural Dynamics, and Materials Conference*, pp. 1–12. ISSN 02734508.
- Volkmer, S., Kuschel, B., Hirschmann, A., Schatz, M., Casey, M. and Montgomery, M., 2012. "Hub Injection Flow Control in a Turbine Exhaust Diffuser". In *Volume 8: Turbomachinery, Parts A, B, and C*. ASME, p. 1713. ISBN 978-0-7918-4474-8. doi:10.1115/GT2012-69713.

## 7. RESPONSIBILITY NOTICE

The authors are the only responsible for the printed material included in this paper.